

Characterization of rejected green banana flour: morphological, structural, and techno-functional properties

Caracterización de la harina de banana verde de rechazo: propiedades morfológicas, estructurales y tecnofuncionales

<https://doi.org/10.15446/rfnam.v78n2.114205>

Nelly Sánchez-Mesa¹, Katherine Manjarres-Pinzón¹, Eduardo Rodríguez-Sandoval^{2*}, Jesus Gil-González² and Guillermo Correa-Londoño³

ABSTRACT

Keywords:

Cavendish
Isotherms
Microstructure
Starch
Thermal properties



Green banana flour (GBF) stands out as a promising raw material for agribusiness due to its techno-functional and nutritional properties. In this study, the characterization of flour obtained from rejected green bananas (*Musa acuminata* AAA, cv. Cavendish) produced in the department of Magdalena, Colombia, located north of the country on the Caribbean coast, was made. Physicochemical, proximate, morphological, structural, and techno-functional parameters were evaluated, as well as their thermal properties and pasting parameters. GBF had a high ash content (2.89%) and a low-fat content (0.6%), which contributes to a high mineral content and flour stability, respectively. The BET mathematical model showed the best fit to describe water absorption in GBF. X-ray diffraction analysis showed a combination of type A and B starch crystallinity. Raman spectroscopy analyses identified characteristic bands, functional groups and molecular interactions related to starch, amylose, and amylopectin (476, 941, and 2,914 cm^{-1}) in the flour. GBF had a pasting temperature around 79.58 °C, good resistance to shear stress at high temperature, and a high tendency to retrogradation. The GBF gelatinization had an enthalpy value of 12.97 J g⁻¹, while the retrogradation enthalpy was 8.19 J g⁻¹. The thermal and pasting values support the starch tendency in GBF to retrograde; this is an attractive property to use GBF as a functional ingredient. This study established the potential of GBF as a promising solution to reduce post-harvest losses of rejected green bananas.


RESUMEN

Palabras clave:

Cavendish
Isotermas
Microestructura
Almidón
Propiedades térmicas

La harina de plátano verde (HBV) se destaca como una materia prima prometedora para la agroindustria por sus propiedades tecnofuncionales y nutricionales. En este estudio, se realizó la caracterización de una harina obtenida de plátano verde de rechazo (*Musa acuminata* AAA, cv. Cavendish) producido en el departamento de Magdalena, Colombia, ubicado al norte del país, en la costa Caribe. Se evaluaron parámetros fisicoquímicos, proximales, morfológicos, estructurales y tecnofuncionales, así como sus propiedades térmicas y parámetros de empastamiento. La HBV tuvo un alto contenido de cenizas (2,89%) y bajo contenido de grasas (0,6%), que contribuyen a un alto contenido mineral y estabilidad, respectivamente. El modelo matemático BET mostró el mejor ajuste para describir la absorción de agua en la HBV. El análisis de difracción de rayos X mostró una combinación de cristalinidad de almidón tipo A y B. Los análisis de espectroscopía Raman identificaron bandas características, grupos funcionales e interacciones moleculares relacionadas con el almidón, la amilosa y la amilopectina (476, 941 y 2.914 cm^{-1}) en la harina. La HBV tuvo una temperatura de gelatinización cercana al 79,58 °C, buena resistencia al esfuerzo cortante a alta temperatura y tendencia a la retrogradación. La gelatinización de la HBV tuvo un valor de entalpía de 12,97 J g⁻¹, mientras que la entalpía de retrogradación fue de 8,19 J g⁻¹. Los valores térmicos y de empastamiento apoyan la tendencia a la retrogradación del almidón en la HBV; esta es una propiedad atractiva para utilizar la HBV como ingrediente funcional. Este estudio estableció el potencial de la HBV como una solución prometedora para reducir las pérdidas postcosecha de plátanos verdes de rechazo.

¹Corporación Natural SIG. Biodiversity, Territory and People Research Group (BIOTEGE). Santa Marta DTCH, Colombia. coordinacion.tecnica@naturalsig.org , directoracientifica@naturalsig.org 

²Departamento de Ingeniería Agrícola y Alimentos, Facultad de Ciencias Agrarias, Universidad Nacional de Colombia, Sede Medellín, Colombia. edrodriguez@unal.edu.co , jhgil@unal.edu.co 

³Departamento de Ciencias Agronómicas, Facultad de Ciencias Agrarias, Universidad Nacional de Colombia, Sede Medellín, Colombia. gcorrea@unal.edu.co 

*Corresponding author

Bananas are one of the most consumed fruits in tropical and subtropical regions (Singh et al. 2016). This fruit is also known for its high nutritional value (Singh et al. 2016). The largest producers of bananas in the world are India, China, and Indonesia, with a representation of 48%; followed by South American countries that participate with 16%: Ecuador and Brazil contribute 5% each, while Colombia ranks ninth with 3% of the world production (Minagricultura 2021).

In 2022, Colombia exported 108 million boxes (20 kg) of bananas from the Caribbean region. The Urabá Antioqueño exported 64 million boxes; while the rest of the Caribbean region, made up of the departments of Magdalena, Guajira, and Cesar sold 44 million boxes abroad (AUGURA 2022). However, there is a percentage of green bananas that do not meet the premium quality requirements of international markets, such as variety, number, size of fingers per bunch, color, appearance, calibration, packaging, and phytosanitary conditions for export (Stanley 2017). This generates economic losses for producers and environmental problems due to the natural degradation of the fruits, which produce toxic gases and leachates that affect water resources and soil quality. Consequently, it is necessary to find alternatives for processing rejected green bananas that favor their conservation and consumption. Due to their high perishability, bananas need to be dried during processing for longer shelf life and storability, as is the case with banana flour (Amarasinghe et al. 2021). The drying process is key and seeks to reduce the weight of the product, facilitating its transport and storage while preserving some of its original properties, such as protein and mineral content. Green banana flour (GBF) preserves the nutritional value of the fruit and also benefits the producer of fresh bananas economically, socially, and environmentally. Its potential as a functional ingredient in food systems could also be explored. Nevertheless, production in banana-growing regions is still artisanal due to the lack of specialized equipment and procedures for its transformation.

Some studies indicate that GBF has a starch content between 58.01 and 81.66% (dry basis) (Wang et al. 2012; Velandia 2019; Kumar et al. 2019; Ahmed et al. 2020; Chang et al. 2022), protein between 2.96 and 5.88%, ash between 1.89 and 3.68%, fat between 0.13 and 4.12% (Kumar et al. 2019; Ahmed et al. 2020; Amarasinghe et

al. 2021; Chang et al. 2022; Alam et al. 2023). Moreover, some technofunctional properties of GBF have been reported, e.g., oil absorption index (OAI) from 1.1 to 1.83 (g g⁻¹), swelling capacity (SC) from 2.7 to 4.92 (g g⁻¹), water absorption index (WAI) from 0.93 to 2.9 (g g⁻¹), and water solubility index (WSI) from 0.28 to 0.36 (g g⁻¹) (Ahmed et al. 2020; Amarasinghe et al. 2021; Alam et al. 2023), Carr's index from 9.38 to 12.06, and Hausner ratio from 1.11 to 1.14 (Alam et al. 2023). These characteristics suggest that GBF is an ingredient suitable for preparing functional products that could help reduce cholesterol and relieve constipation (Anyasi et al. 2015). In addition, GBF could be used to supplement bakery products, pasta, cookies, and baby foods (Aurore et al. 2009). The functionality of starch—the main component of GBF—can vary even within the same cultivar depending on environmental factors; there are structural and functional differences in green banana flour according to its origin and cultivar (Kumar et al. 2019). This research aims to characterize the flour obtained from rejected green banana (*Musa acuminata* AAA, cv. Cavendish) produced in the department of Magdalena, Colombia, by determining physicochemical, morphological, thermal, pasting, structural, and technofunctional properties. This could lay the foundations to establish its potential as a functional ingredient in the food industry.

MATERIALS AND METHODS

Plant material

The plant material was rejected green banana (*Musa acuminata* AAA, cv. Cavendish) from the municipalities of Aracataca, Ciénaga, and Zona Bananera (Department of Magdalena, Colombia). Bananas' ripeness stage was between 1 and 2 (green) (Ortega 2016; Jaramillo-Garcés et al. 2023).

Characterization of the raw material

The soluble solids content (°Brix), pH, titratable acidity, and moisture content were determined according to AOAC (2005) to characterize green banana pulp. Its water activity (a_w) was measured using a dew point hygrometer (AquaLab 3TE Series, Decagon Devices, Inc., Pullman WA, Pullman WA, USA) (Manjarres-Pinzón et al. 2024).

Obtaining GBF

Slices of the pulp with a thickness of 5 mm were obtained and immersed in an anti-browning solution. Subsequently,

they were dried in a convection oven (UF750, Memmert, Germany) at 55 °C for 15 h, then ground and stored at room temperature (25 °C) in metalized bags until further analysis (Jaramillo-Garcés et al. 2023).

Physicochemical and proximate characterization of GBF

The following physicochemical parameters of the GBF were determined: pH, titratable acidity, moisture content, and water activity (a_w) (AOAC 2005). Color parameters were determined according to the CIELAB color scale: L^* =0 (black) to L^* =100 (white), $-a^*$ (green) to $+a^*$ (red), and $-b^*$ (blue) to $+b^*$ (yellow). Color parameters L^* , a^* , b^* , chroma (C^*), and hue angle (h^*) were measured; in addition, the yellowness (YI) and whiteness (WI) indices were calculated using Equations (1) and (2) proposed by Borneo et al. (2016), respectively.

$$YI = \frac{142.86b}{L} \quad (1)$$

$$WI = 100 - ((100 - L)^2 + a^2 + b^2)^{1/2} \quad (2)$$

GBF sorption isotherms were determined using the static gravimetric method, as described by Gutiérrez et al. (2018). The moisture content of the samples was measured after reaching equilibrium at specific water activities maintained using saturated salt solutions, including potassium acetate (CH_3COOK), magnesium chloride ($MgCl_2$), potassium carbonate (K_2CO_3), magnesium nitrate ($Mg(NO_3)_2$), potassium iodide (KI), sodium chloride (NaCl), and potassium chloride (KCl). These experiments were performed at temperatures of 15, 25, and 35 °C. Thymol (0.5 g) was added to containers with an $a_w > 0.5$ to prevent microbial growth. Initial sample weights were recorded, and final weights were measured after 40 days when equilibrium was reached. Sorption isotherms were fitted using several models, including GAB (Guggenheim-Anderson-de Boer), BET (Brunauer-Emmett-Teller), SMITH and OSWIN. Non-linear regression was used to calculate model parameters, minimizing the root mean square error between the experimental data and the model predictions. The moisture content of the sample was determined after having reached equilibrium with the air of known relative moisture (a_w between 0.234 and 0.859) at 15, 25, and 35 °C. Proximate analyses of GBF were conducted according to AOAC (2005) to determine levels of crude

protein, ash, fat, native starch, and total fiber. The amylose content was determined by adding 10 mg of sample (dry basis) to 10 mL of DMSO (95% w/w). The suspension was heated in a water bath at 80 °C for 15 min under constant stirring. The mixture was cooled to room temperature and allowed to stand for 15 min. A solution of I_2/KI (100 μ L) and distilled water (1,800 μ L) was then added to 100 μ L of the sample and allowed to react for 20 min in the dark. Finally, the absorbance was measured at a wavelength of 620 nm in a spectrophotometer (Thermo Scientific, Genesys 10S). The calibration curve was established using potato amylose and maize amylopectin standards at concentrations between 0-100% w/v (Figuroa-Flórez et al. 2024).

Morphological characterization of GBF

The birefringence of GBF samples was determined by observation under polarized light of GBF suspensions in deionized water; a binocular microscope (Leica, DM1000 led, Japan) with 40X magnification and equipped with a digital camera (Leica, ICC50W, Japan) was employed. The granular morphology of the GBF samples was evaluated with a Scanning Electron Microscope (SEM) (Zeiss, EVO MA10). Samples were placed in a sample holder with electroconductive carbon tape and covered with a platinum/gold alloy. The observation conditions of the samples were established at 15 kV, 30 mA, and magnifications of 400X and 800X.

Structural characterization of GBF

Particle size distribution was estimated by light scattering using a particle analyzer (Mastersizer 3000E, Malvern Instruments Ltd., UK); a refractive index value of 1.52, an absorption index of 0.05, and a mode of operation using air as a dispersing agent were employed. Particle size was expressed as a function of mean diameters $D(10)$, $D(50)$, $D(90)$, $D[3;2]$, and $D[4;3]$. The diffraction patterns of the samples were obtained on an X-ray diffractometer (X'Pert Pro- MPD, Panalytical, Italy). Intensities were detected in a range of Bragg 2θ angles of 5-70°, with a current of 30 mA and 40 kV of operation. The degree of crystallinity was estimated from the ratio of the crystalline areas and the total area (crystalline + amorphous) obtained by data processing using Matlab R2019a (MathWorks, R2019a, USA) (Padhi and Dwivedi 2022). The data were then smoothed using the Savitzky-Golay algorithm and the deconvolution process was developed using the Gaussian

function in the 5–30° region (Figueroa-Flórez et al. 2024). The intensity values of the XRD patterns were normalized by dividing them by the maximum intensity of the most prominent peak. Crystalline peaks were identified using a peak-finding algorithm in Matlab, which detected local maxima above a predefined threshold. The areas under the crystalline peaks were then integrated. The Raman spectra of the samples were collected using a Raman spectrometer (Horiba Scientific, LabRAM HR Evolution) with a 600 nm laser source, 5 mW power, 1 s acquisition time, and a 50X objective lens.

Thermal properties and pasting parameters of GBF

The thermal properties of the flour samples were determined using a differential scanning calorimeter (DSC 250, TA Instruments, USA). Flour/water suspensions (3.4 mg flour/10 μ L water) were prepared in aluminum capsules, sealed, and kept refrigerated for 24 h. The thermal properties of each treatment were evaluated using a heating ramp from 30 to 120 °C at 10 °C min⁻¹; followed by a cooling ramp down to 30 °C at 25 °C min⁻¹. Subsequently, the capsule containing the gelatinized starch was stored at refrigeration temperature (4 °C); after 15 days, the thermal properties were determined under the same operating parameters of the DSC. An empty aluminum capsule was used as a reference. The following parameters were obtained from the thermograms and the TA Universal Analysis software (TA Instruments, USA): onset temperature (To), peak temperature (Tp), end temperature (Tf), gelatinization enthalpy (J g⁻¹) (ΔH), and retrogradation enthalpy (J g⁻¹) (ΔH_r).

Pasting parameters were measured on a micro visco-amylograph (Brabender GmbH & Co. KG, Duisburg, Germany) coupled to a thermostat bath (F-12ED, Julabo, Baden-Wuerttemberg, Germany). The GBF/water suspension (5 g GBF/110 mL water) was heated from 30 to 95 °C at a rate of 7.5 °C min⁻¹, temperature was maintained at 95 °C for 5 min; subsequently, the sample was cooled to 50 °C at a rate of 7.5 °C min⁻¹; finally, the temperature was maintained for 5 min. Viscosities were recorded in Brabender Units (BU) and parameters such as pasting temperature, peak viscosity, breakdown, setback, and final viscosity were determined.

Techno-functional properties of GBF

The oil absorption index (OAI), swelling capacity (SC),

water absorption index (WAI), and water solubility index (WSI) were determined according to the methodologies employed by Rodríguez-Sandoval et al. (2014). The bulk density was calculated by weighing 2 g of flour and measuring its volume in a 10 mL test tube. Subsequently, in the same tube, manual vibration was applied to the flour, and the volume was measured again to calculate the compacted density. The Carr index and Hausner ratio were calculated with bulk density and tapped density using the equations proposed by Moravkar et al. (2020). Finally, to determine the minimum gelation concentration (MGC) in test tubes, aqueous suspensions of GBF (5 mL) were prepared at concentrations of 2, 4, 6, 8, 10, 12, 14, 16, 18, 20 and 22%. Subsequently, the suspensions were vortexed for 30 seconds at 3,000 rpm and brought to a water bath (with stirring) for 45 min at 85 °C. The suspensions were then cooled with ice-water and stored at 4 °C for 24 h. The minimum gelation concentration was determined as the concentration at which the sample did not slip from the inverted test tube.

Statistical Analysis

All experiments were done in triplicate. The mean and standard deviation of all properties were calculated using Statgraphics (Centurion XVIII). In the isotherms, model parameters were estimated using the DATAFIT 9 non-linear regression software (Oakdale Engineering).

RESULTS AND DISCUSSION

Characterization of the raw material

Results of the physicochemical analysis of rejected green banana pulp are shown in Table 1. Its physicochemical parameters vary depending on cultivar, ripening stages, and environmental conditions (Melgarejo 2012). However, some of the values obtained for the Cavendish cultivar coincide with the parameters reported by different authors for other green-ripening banana cultivars (Ahmed et al. 2020; Anyasi et al. 2015). In particular, the pH and acidity values obtained from the pulp agree with the results reported by De Souza et al. (2021) for the same cultivar; however, substantial differences were obtained with respect to the soluble solids content (1.39 compared to values close to 11%). This could be associated with the ripening stage of the fruit. In this study, it was approximately 11 (Brix/acidity), which indicates that the fruits used to obtain GBF were at the first stage (Khoozani et al. 2019). Acidity is closely

related to the taste of the fruit (Ahmed et al. 2020) and is mainly represented by malic, citric, and oxalic acids; the latter contributes significantly to the astringency of the green fruit. High moisture and a_w values indicate

microbiological instability; however, this can be mitigated by the low acidity and pH values found in the pulp. With a moisture of 74.06%, the net dry matter weight (flour) is expected to be around 26%.

Table 1. Physicochemical characterization of fresh green banana pulp.

Analysis	Mean \pm standard deviation
Moisture (%)	74.06 \pm 0.98
a_w	0.983 \pm 0.01
pH	5.61 \pm 0.13
Acidity (%) [*]	0.13 \pm 0.07
°Brix	1.39 \pm 0.30

^{*}Expressed as a percentage of malic acid.

Physicochemical and proximate characterization of GBF
GBF was obtained with a yield of 10% and with a moisture content of 7.2% (Table 2). This value meets the quality standard limits (<10%) for banana flours in Colombia (ICONTEC 2020) and is lower than that recommended for fruit powders (13%). A low-moisture product is considered stable against microbial spoilage (Pragati et al. 2014).

Moisture content and a_w were similar to those reported in GBF dehydrated by convection at 50 °C (5.09% and 0.25) (Khoozani et al. 2019). These parameters, which assess the availability of water for use by microorganisms, are indicators of the physical, chemical, and microbial stability of the product and, therefore, the shelf life of food (Khoozani et al. 2019).

Table 2. Physicochemical results for green banana flour.

Analysis	Mean \pm standard deviation
Moisture (%) ²	7.2 \pm 0.8
Acidity ¹	0.16 \pm 0.04
pH	5.36 \pm 0.15
a_w	0.227 \pm 0.031
Native starch (%) ²	81.95 \pm 4.45
Amylose (%)	23.94 \pm 1.27
Crude protein content (%) ²	4.45 \pm 0.35
Ash (%) ²	2.89 \pm 0.54
Fat content (%) ²	0.6 \pm 0.14
Total Dietary Fiber (%) ²	7.85 \pm 1.06
Color	
L [*]	44.88 \pm 6.03
a [*]	1.24 \pm 0.29
b [*]	8.46 \pm 0.94
C [*]	8.56 \pm 0.94
WI	44.20 \pm 0.94
YI	27.06 \pm 1.96
h [*]	81.58 \pm 1.98

Table 2

Analysis	Mean \pm standard deviation
Particle Size	
D (10) (μm)	29.4 \pm 7.2
D (50) (μm)	230.1 \pm 89.2
D (90) (μm)	1,377.1 \pm 213.0
D [3;2] (μm)	75.6 \pm 16.8
D [4;3] (μm)	487.3 \pm 91.3

¹Expressed as a percentage of malic acid. ²Results expressed on a dry basis. WI: whiteness index. YI: yellowness index. h*: Hue angle.

The values of pH and acidity in GBF are low because they are related to the ripeness state of the raw material (green). The presence of various oxo acids has been reported in the pulp of green bananas; oxalic, malic, and citric acids contribute to the acidity of green banana flour (Drapal et al. 2024).

The ash content was high compared to the reported values (1.89-3.25%) in GBF obtained from different banana varieties (Kumar et al. 2019). The quality of the flour depends on the ash content, which provides the Cavendish variety with minerals, especially sodium and magnesium (Pragati et al. 2014). The fat content was less than 0.50 g 100 g⁻¹, thus favoring the stability of the flour because oxidative rancidity reactions are not favored. GBF samples have a starch content of more than 80%, which is higher than that reported for other cultivars (Ahmed et al. 2020; Chang et al. 2022), and an amylose percentage similar to that reported in the literature (Campuzano et al. 2018; Chang et al. 2022).

Color is a sensory attribute that impacts the degree of consumer acceptance. Variability in the luminosity (L*) of GBF samples could be associated with darkening reactions caused by the action of polyphenol oxidase (Zamudio et al. 2010), or by non-enzymatic browning associated with the reaction of starch with proteins during drying. Furthermore, the values of a* —which represents the coordinate of the red-green colors—, and b* —which represents the coordinates of the yellow-blue colors— were 1.24 \pm 0.29 and 8.46 \pm 0.94, respectively. These values agree with a reddish (a*) and yellowish (b*) hue of the flour. This result, as well as the C* values, could be related to the presence of carotenes and other pigments in the pulp and enzymatic reactions (Campuzano et al. 2018). Likewise, the C* value

of food increases along with the concentration of pigment and decreases markedly as the samples darken.

The hue (h*) of GBF tends towards yellow, with values close to 90°. In addition, chromaticity resulted in 8.56 \pm 0.94, with a more saturated coloration. The whiteness index (WI) (44.20 \pm 0.94) and the yellowness index (YI) (27.06 \pm 1.96) are the result of the effect of temperature on the color and quality of GBF. High WI and low YI values are preferable because incorporating flours into a food matrix (e.g., baking) should not affect the color of the final product (Padhi and Dwivedi 2022). Kumar et al. (2019) reported higher WI (>80) and YI (15 to 40) values in GBF obtained from different banana cultivars.

The particle size distribution of GBF is shown in Table 2. The average values of D (10), D (50), and D (90) represent GBF particles smaller than the average particle size in flour samples (i.e., 10, 50, and 90%) (Wu et al. 2022). Results show a fraction of starch granules corresponding to type A (5-60 μm) (Vogel et al. 2018). Although the values of D (50) and D [4;3] suggest a high proportion of small particles related to intense milling conditions, 90% of the mass of the particles has a size equal to or less than 1,377.1 μm , and the remaining 10% of the particles are larger than that, thus indicating a heterogeneous distribution. These values are important considering that in powdered products used in food preparation, a higher degree of solubility and dispersibility is observed when they have smaller and finer particles. When the specific surface area is important, the mean Sauter diameter D [3;2] is measured, as it is more sensitive to the presence of fine particles in the size distribution. Whereas the volume means diameter D [4;3] reflects the size of the particles that make up the bulk of the sample volume and

is more sensitive to the presence of large particles in the size distribution.

Isotherms and sorption models

Four mathematical models (GAB, BET, SMITH, and OSWIN) were adjusted to describe the water sorption behavior of GBF at 15, 25, and 35 °C, and some indices were calculated to determine the quality of the adjustment. Figure 1 shows the BET working isotherms obtained for GBF at different temperatures. They show the relationship

between water activity and equilibrium moisture content. The isotherms obtained are sigmoidal type II; these are common in foods such as fruits and vegetables, and in foods that have a high starch content (Ayala-Aponte 2016). According to Cardoso and Pena (2014), these types of isotherms are models with an adequate level of adjustment for GBF and can also indicate a porous structure of the flour. Similarly, the equilibrium moisture increased with the increase in the a_w value; several authors found a similar behavior (Bezerra et al. 2013; Susilo et al. 2019).

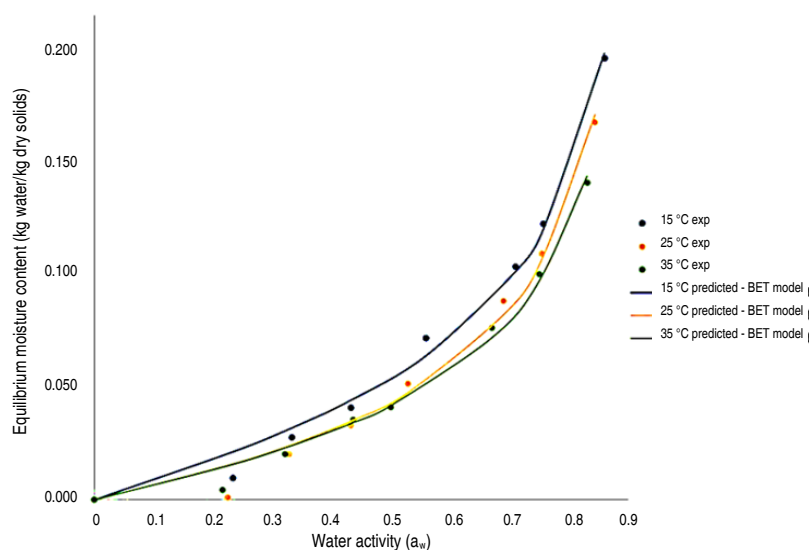


Figure 1. Moisture adsorption isotherms of green banana flour at 15, 25, and 35 °C.

Starch sorption may be influenced by hydrogen bonds between water molecules and available hydroxyl groups on amylose and amylopectin chains, especially in amorphous areas and on crystal surfaces (Aguirre-Cruz et al. 2010). The crystalline regions of the starch show a lower permeability to solvents. As a result, the presence of water acts as a plasticizer of the amorphous areas and affects the starch structure.

The exponential behavior of isotherms for a_w levels greater than 0.6 indicated that GBF peaked at 0.20, 0.17, and 0.14 kg water/kg dry solids at 15, 25, and 35 °C, respectively. Some authors indicate that relative humidity (RH) values below 0.60 guarantee the stability of some products under storage conditions (Gutiérrez et al. 2018; Cardoso and Pena 2014).

The adjusted parameters of the used sorption models are presented in Table 3. The BET, OSWIN, and SMITH models had the lowest CME and E_{RMS} values, respectively. This suggests that they have the best fit to the experimental data and good accuracy of the models in predicting data compared to the GAB model, which showed higher CME and E_{RMS} values. It was also observed that the BET and OSWIN models presented low P values, thus indicating a statistically significant adjustment to the experimental data. Similarly, different trends are observed when examining the predictor variables of the models as a function of temperature. In GAB and BET, they presented the highest W_m value (moisture content of the monolayer) at 35 °C, indicating that water sorption is more pronounced at this temperature. Likewise, C showed an increase in BET at 35 °C, suggesting a higher rate of water adsorption. In

the case of the OSWIN model, the value of “a” decreases as the temperature increases, which may be due to a lower water adsorption capacity at higher temperatures.

Finally, in the SMITH model, the parameters “a” and “b” appear to be independent of temperature, as they remained constant under the three evaluated conditions.

Table 3. Estimated parameters and adjustment indices of various sorption models for banana flour.

Model	Constant	15 °C	25 °C	35 °C
GAB $M = W_m \frac{Ca_w}{(1 - Ka_w)(1 - Ka_w + CKa_w)}$	Wm	0.87890	0.68664	1.01997
	C	0.17383	0.19410	0.11791
	k	0.39458	0.42454	0.39240
	R ²	0.92888	0.94260	0.94810
	P	0.00563	0.00491	0.00307
	CME	0.00141	0.00098	0.00061
	E _{RMS}	0.00035	0.00031	0.00019
BET $M = W_m \frac{Ca_w}{(1 - a_w)(1 - a_w + Ca_w)}$	Wm	0.29957	0.14209	0.16401
	C	0.28664	0.28664	0.37861
	R ²	0.99177	0.98797	0.99116
	P	0.00026	0.00030	0.00016
	CME	2.586x10 ⁻⁰⁵	5.081x10 ⁻⁰⁵	2.586x10 ⁻⁰⁵
	E _{RMS}	1.608x10 ⁻⁰⁵	1.906x10 ⁻⁰⁵	9.696x10 ⁻⁰⁶
SMITH $M = a - b \ln(1 - a_w)$	a	1.000x10 ⁻⁰²	1.000x10 ⁻⁰²	1.000x10 ⁻⁰²
	b	0.09288	0.08223	0.07425
	R ²	0.99113	0.9937	0.9961
	CME	5.6999x10 ⁻⁰⁴	5.5351x10 ⁻⁴	3.6595x10 ⁻⁴
	E _{RMS}	1.4250x10 ⁻⁰⁴	0.000172972	1.1436x10 ⁻⁴
OSWIN $M = a \left[\frac{a_w}{1 - a_w} \right]^b$	a	0.05352	0.04363	0.04187
	b	0.73784	0.82608	0.79217
	R ²	0.99004	0.9876	0.9901
	CME	7.13035x10 ⁻⁰⁵	6.01137x10 ⁻⁰⁵	3.23386x10 ⁻⁰⁵
	E _{RMS}	1.78259x10 ⁻⁰⁵	1.87855x10 ⁻⁰⁵	1.01058x10 ⁻⁰⁵

M: equilibrium moisture content; a_w: water activity; a, b, C and k: model parameters estimated by least squares; Wm: moisture content of the monolayer.

The BET model for equilibrium moisture content showed better fits with respect to the experimental data, it presents the lowest CME and E_{RMS} values for the temperatures tested.

The data obtained showed that GBF tends to absorb more water with increasing temperature at a certain aqueous activity. This can be attributed to the increased mobility of water molecules and the adsorption energy of water as temperature increases (Ayala-Aponte 2016). In addition, the mathematical models GAB, BET, and OSWIN showed changes in their parameters as a function of temperature,

indicating a significant dependence of GBF sorption behavior on temperature.

Birefringence and Scanning Electron Microscopy (SEM)

Micrographs obtained by polarized light microscopy (Figure 2) show elongated and oval-shaped granules, similar to those found by Chávez-Salazar et al. (2017). In addition, the formation of the Maltese cross indicates that there is a high degree of molecular orientation within the granule, and that these did not undergo internal decomposition or gelatinization during the drying and

grinding process (Chávez-Salazar et al. 2017). The Maltese cross also indicates that the starch is native, and that the crystal arrangement is anisotropic.

Generally, birefringence studies are linked to the study of starch gelatinization, a process by which starch granules

absorb water when heated to a temperature close to 65 °C (depending on the starch) and a dispersion above 30% moisture content. Once the granules reach their maximum volume, they partially break down and leach amylose and amylopectin, leading to the loss of the original organization of the granule and birefringence.

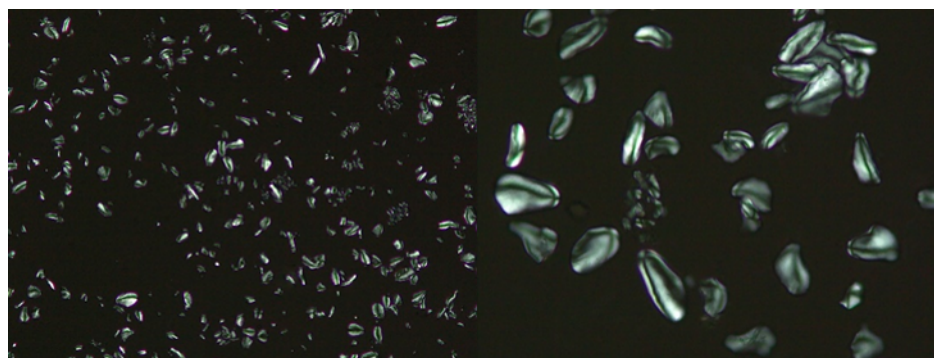


Figure 2. Polarized light microscopy of the starch granules present in GBF observed with 10X and 40X lenses.

Figure 3 shows GBF morphology at 400X and 800X magnification. Granules of unequal sizes, between 19 and 76 µm, and irregular shapes were observed; the elongated shape was predominant. The shape of these granules was similar to that found by Chang et al. (2022) in 6 varieties of green bananas from Tanzania, also finding

a variation in sizes between 25.27 and 65.83 µm. The image also showed a layer that covers the granules and is mainly composed of pectin and cellulose (Salvador et al. 2000); moreover, the granules exhibited their complete shape because starch did not disintegrate during drying.

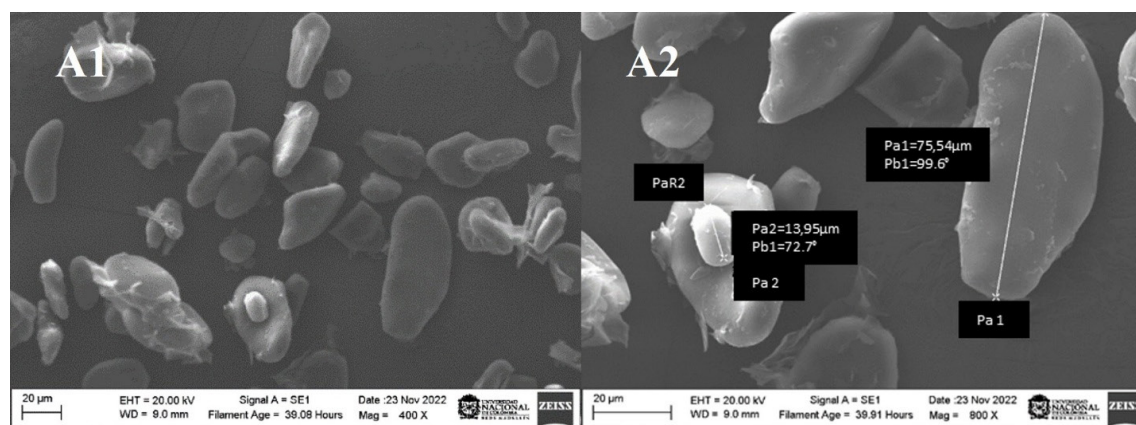


Figure 3. Scanning electron micrographs of GBF (A1:400X, A2:800X).

X-ray diffraction and RAMAN Spectrum

Green banana pulp contains up to 70-80% starch by dry weight; starches are generally classified into three types: A, B, and C according to the type of X-ray diffraction pattern shown by their crystalline lamellae. The type of diffraction pattern depends mainly on the

arrangement of amylopectin double helices chains and the agronomic and environmental conditions of the crop (Vega-Rojas et al. 2021). Kumar et al. (2019) reported that banana flour made of the Grand Naine, Monthan, and Saba varieties have a crystallinity of 12.22, 15.31, and 9.38%, respectively. Crystallinity will vary according

to the banana cultivar used for the analysis and to the influence of the chemical composition of the flour, i.e., ash, lipid, protein, and fiber content (Padhi et al. 2022).

The X-ray diffraction pattern and Raman spectrum for the GBF sample are shown in Figure 4. The diffractogram (Figure 4A) presented the characteristics of a mixture of type A and B starch crystallinity with strong peaks at approximately 15, 18, and 23°, similar to that reported by Kumar et al. (2019) in five GBFs obtained from different banana varieties. The percentage of crystallinity calculated for GBF was 31.30%, a value similar (29.29%) to that reported by Campuzano et al. (2018) in GBF from the cultivar *Musa acuminata* (AAA), var. Cavendish.

In the Raman spectrum (Figure 4B), spectral bands between 400 and 800 cm^{-1} are attributed to the bending vibrations of C–C–C and C–C–O and torsional vibrations C–O (Mir and Bosco 2014). Some characteristic starch bands have been reported at 400, 430, 469, 518, 708, and 758 cm^{-1} (Czekus et al. 2019). The band at 476 cm^{-1} is considered typical of the starch skeleton. The vibrations originating from the α -1,4 glycosidic bonds can be observed as strong Raman bands in the region of 920–960 cm^{-1} ; in fact, the band observed at 941 cm^{-1} has been assigned to the skeletal mode vibrations of the α -1,4 glycosidic bond (C–O–C) in starch (Mir and Bosco 2014). Finally, the strong band at 2914 cm^{-1} has been related to the symmetrical and asymmetrical stretching of the C–H

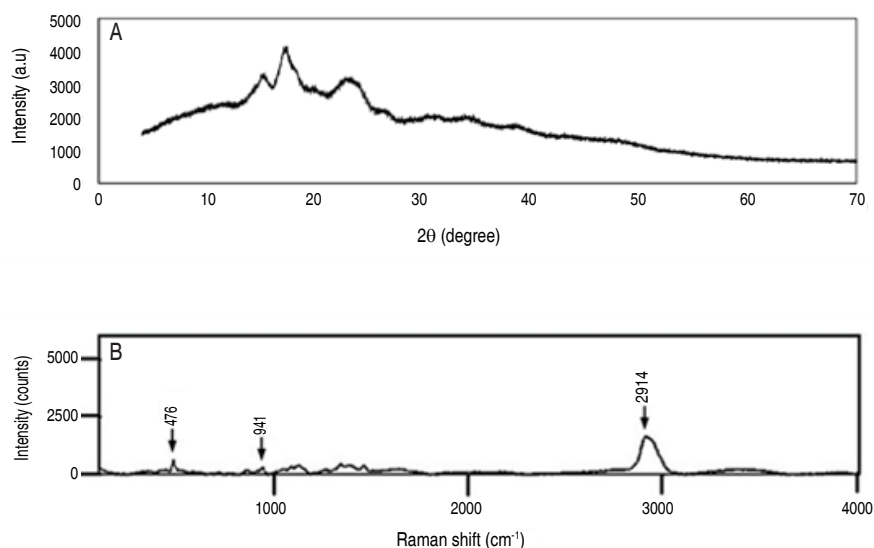


Figure 4. GBF X-ray diffraction (A) and Raman spectroscopy (B).

bond. According to Kizil et al. (2002), intensity changes in this range can be largely attributed to variations in the amount of amylose and amylopectin present in starches.

Thermal and pasting properties of GBF

Results obtained from differential calorimetry analysis of GBF are presented in Table 4. The gelatinization initiation and termination temperature ranged between 74.93±0.15 and 82.17±0.32 °C, respectively, with a peak or gelatinization temperature of 78.35±0.21 °C and a gelatinization enthalpy of 12.97±1.55 J g⁻¹. It has been reported that peaks with a narrow temperature range indicate lower heterogeneity of amylopectin crystals

because they become disorganized during heating in a lower temperature range. Similar values were reported by Tribess et al. (2009) for different GBFs obtained from *Musa acuminata* (AAA), cv. Cavendish, under different drying conditions. The Tp and ΔHg values were lower and ranged from 67.95±0.31 to 68.63±0.28 °C and from 9.04±1.71 J g⁻¹ to 11.63±1.74 J g⁻¹, respectively. These differences occur because the thermal transitions of starch depend on factors typical of the grain, such as its shape, the type of association of amylose molecules with amylopectin and lipids (complexes), and the alignment of hydrogen bonds in the crystalline region, among others.

During retrogradation, water-dispersed amylose and amylopectin molecules rearrange during storage to form ordered structures. The retrogradation tendency of gelatinized starches is commonly measured by thermal analysis (DSC). The amount of energy required to dissociate the annealed amylopectin molecules after 15 days of storage in GBF was $8.19 \pm 1.37 \text{ J g}^{-1}$, lower than that observed during GBF gelatinization. However, it indicates the high content of retrograde starch that can be obtained from GBF. Additionally, lower transition temperatures (T_{or} , T_{pr} , and T_{fr}) were compared to those obtained in gelatinization, indicating that the reassociation of amylopectin during storage is not similar to the ordering present in the native state.

Pasting parameters play an important role in the choice of flour, since they make it possible to analyze the behavior of a suspension formed by flour and water in a heating/cooling cycle. These properties depend on the type of processing used to obtain the flour, the amylose, protein and lipid

content and the stiffness of the starch granules, which also influence their swelling capacity (Devi and Haripriya 2014). Moreover, these properties make it possible to determine the function of flour in the food industry to be used as a thickener, binder, or for any other use.

The results obtained for GBF are summarized in Table 4. The found pasting temperature was similar to that reported (72.51°C) by Chang et al. (2022). The pasting temperature is affected by the presence of other flour components that compete for water, such as proteins. The flour was consistent after cooling and reached a higher final viscosity value compared to the peak viscosity. It also exhibited good shear strength at high temperature (95°C), with a decrease in peak viscosity of approximately 6 BU. Finally, the setback value may indicate a tendency of flour to gel formation or rapid retrogradation associated with amylose (López-Ochoa et al. 2022). This could be associated with a high content

Table 4. Thermal and pasting properties of GBF.

Pasting Properties	Mean \pm standard deviation
Peak Viscosity (BU)	113.38 ± 5.35
Breakdown (BU)	5.75 ± 1.73
Setback (BU)	18.88 ± 4.27
Final viscosity (BU)	137.38 ± 14.15
Pasting temperature ($^\circ\text{C}$)	79.58 ± 0.61
Thermal properties (gelatinization, day 0)	
T_o ($^\circ\text{C}$)	74.93 ± 0.15
T_p ($^\circ\text{C}$)	78.35 ± 0.21
T_f ($^\circ\text{C}$)	82.17 ± 0.32
ΔH_g (J g^{-1})	12.97 ± 1.55
Thermal properties (retrogradation, day 20)	
T_{or} ($^\circ\text{C}$)	46.11 ± 1.18
T_{pr} ($^\circ\text{C}$)	65.85 ± 0.41
T_{fr} ($^\circ\text{C}$)	78.89 ± 0.70
ΔH_r (J g^{-1})	8.19 ± 1.37

*BU: Brabender units.

of resistant starch in green banana flour, as reported by several authors (Kumar et al. 2019; Khoozani et al. 2019).

Techno-functional properties of GBF

The influence of the flow and compression properties of banana flour on its quality was evaluated (Table 5). The

Hausner ratio (HR) and the Carr index (CI) were determined, which are obtained from the apparent and compacted densities of the material. HR is a measure of the degree of cohesion between particles of the powder, while CI is a measure of the variation of the density of the material when subjected to an external force. The results showed low fluidity and a

tendency to agglomeration, which could negatively affect its handling and processing. Banana flour was also found to have moderate compressibility. Similar results were reported by Grisi et al. (2021) in flour obtained from juca (*Libidibia ferrea*) and higher compared to GBF results from different drying methods (Alam et al. 2023). This feature can make it difficult to accurately dose flour in production processes and could compromise the performance and quality of the final product. Findings suggest that drying conditions, adding anti-agglomerating agents, among other possible solutions, are required in banana flour to obtain more uniform particles and optimize its use in the food industry. Similarly, Table 5 shows the results of the hydration, solubility, and gelling properties of GBF. In flours, the water absorption index (WAI) is an indicator of the yield of fresh dough, while the oil absorption index (OAI) is related to the hydrophobic character of the starch present in it. The content and nature of starch, the amount of protein and insoluble fiber in flour can influence those values.

Table 5. Techno-functional properties of rejected green banana flour.

Parameters	Value
Hausner ratio	1.340±0.069
Carr Index	25.202±3.781
WAI (g g ⁻¹)	3.060±0.158
WSI (g g ⁻¹)	6.326±0.730
SC (g g ⁻¹)	3.269±0.173
OAI (g g ⁻¹)	0.760±0.071
MGC (%)	6±0

Khoozani et al. (2019) reported similar WAI values (3.01) for GBF obtained at 50 °C but found higher OAI values (2.77) compared to those obtained in this study.

While the WSI is related to the number of soluble solids in the flour, SC represents the interaction between the starch chains within the amorphous and crystalline domains of the starch granule and is influenced by the characteristics of amylose and amylopectin. Bezerra et al. (2013) found lower WSI values (1.22-1.9 g g⁻¹) in GBF obtained at 80 and 90 °C. In contrast, the GBF SC values were lower than those reported by Ortega (2016) and Bezerra et al. (2013), although closer to those reported by Padhi and Dwivedi (2022), who found a SC of 2.54±0.45. A low SC value indicates the presence of higher binding forces

inside the starch granules and a higher importance of the amylose-lipid complexes, but the latter would not be the case due to the low lipid content of the samples. Finally, the value obtained for MGC indicated gelling properties of GBF at a relatively low concentration (6%), which could be advantageous in the formulation of food products that require a gelatinous texture, such as soups, sauces, and desserts, among others.

CONCLUSION

Green banana flour (GBF) possesses techno-functional, physicochemical, physical, structural, and morphological properties that make it a suitable food ingredient for use across a wide spectrum of the food industry. Its fat content was low, which was beneficial to the stability of the flour. The whiteness index and the yellowness index of GBF were intermediate, indicating that this flour can be incorporated into a food matrix without significantly affecting its color. Although the values of D(50) and D[4;3] indicate a high proportion of small particles, 90% of the particle mass is equal to or smaller than 1,377.1 µm; the remaining 10% are larger, thus indicating a heterogeneous distribution. The starch granules of GBF are elongated and oval-shaped. Furthermore, the Hausner ratio and Carr index results showed low fluidity and a tendency to agglomerate, which could adversely affect its handling and processing. Moderate compressibility was also found. GBF also exhibited consistency after cooling, high temperature shear strength, and thermal and pasting values, supporting starch retrogradation behavior, which is attractive for use as a functional ingredient in a variety of foods.

During the drying and milling process, starch granules maintained their integrity without undergoing decomposition or gelatinization. This was corroborated by SEM and Raman, which showed characteristic bands of starch structure. In addition, the BET, OSWIN and SMITH models have the best fits to the experimental data and the accuracy of the models in predicting the data is good when compared to the GAB model. Better fits to the experimental data were obtained with the BET model for equilibrium moisture content. Moreover, it was determined that GBF presented a crystallinity of 31.30%, corresponding to a combination of type A and B starches in its composition. This research contributes to the growing body of knowledge on the valorization of rejected green bananas by transforming them into a valuable food ingredient. The detailed characterization of GBF's

properties provides a scientific basis for its application in the food industry. Further research is needed to evaluate other important nutritional properties, such as digestibility, resistant starch content, and antioxidant activity, as well as the performance of GBF in specific food matrices, including bakery products, pasta, and gluten-free formulations.

ACKNOWLEDGMENTS

Tecniban project BPIN code 2020000100698 and Hermes code 51045, Corporación Natural SIG, and Universidad Nacional de Colombia – Medellín Headquarters. K. Manjarres-Pinzon thanks Minciencias Call 935 for contract CT 195-2023.

CONFLICT OF INTERESTS

The authors declare that they have no known competing financial interests or personal relationships that could have appeared to influence the work reported in this paper.

REFERENCES

- Aguirre-Cruz A, Alvarez-Castillo A, Castrejón-Rosales T, Carmona-García R et al (2010) Moisture adsorption behavior of banana flours (*Musa paradisiaca*) unmodified and modified by acid-treatment. *Starch-Stärke* 62: 658-666. <https://doi.org/10.1002/star.201000028>
- Ahmed ZFR, Taha EMA, Abdelkareem NAA and Mohamed WM (2020) Postharvest properties of unripe bananas and the potential of producing economic nutritious products. *International Journal of Fruit Science* 20: S995-S1014. <https://doi.org/10.1080/15538362.2020.1774469>
- Alam M, Biswas M, Hasan MM, Hossain MF, Zahid MA, Al-Reza MS and Islam T (2023) Quality attributes of the developed banana flour: Effects of drying methods. *Heliyon* 9(2023): e18312 <https://doi.org/10.1016/j.heliyon.2023.e18312>
- Amarasinghe NK, Wickramasinghe I, Wijesekara I, Thilakarathna G and Deyalage ST (2021) Functional, physicochemical, and antioxidant properties of flour and cookies from two different banana varieties (*Musa acuminata* cv. Pisang awak and *Musa acuminata* cv. Red dacca). *International Journal of Food Science*, 2021(1): 6681687. <https://doi.org/10.1155/2021/6681687>
- Anyasi TA, Jideani AIO and Mchau GA (2015) Morphological, physicochemical, and antioxidant profile of noncommercial banana cultivars. *Food Science and Nutrition* 3: 221–232. <https://doi.org/10.1002/fsn3.208>
- AOAC - Association of Official Analytical Chemists (2005) Official methods of analysis of the AOAC International. 18th edition. Gaithersburg, MD.
- AUGURA – Asociación de bananeros de Colombia (2022) Coyuntura bananera, análisis del mercado del banano. <https://augura.com.co/wp-content/uploads/2022/04/COYUNTURA-BANANERA-2021.pdf>
- Aurore G, Parfait B and Fährsmane L (2009) Bananas, raw materials for making processed food products. *Trends in Food Science and Technology* 20: 78–91. <https://doi.org/10.1016/J.TIFS.2008.10.003>
- Ayala-Aponte AA (2016) Thermodynamic properties of moisture sorption in cassava flour. *Dyna* 83: 138-144. <https://doi.org/10.15446/dyna.v83n197.51543>
- Bezerra CV, Amante ER, de Oliveira DC, Rodrigues AM and da Silva LHM (2013) Green banana (*Musa cavendishii*) flour obtained in spouted bed—Effect of drying on physico-chemical, functional and morphological characteristics of the starch. *Industrial Crops and Products* 41: 241-249. <https://doi.org/10.1016/j.indcrop.2012.04.035>
- Borneo R, Alba N and Aguirre A (2016) New films based on triticale flour: Properties and effects of storage time. *Journal of Cereal Science* 68: 82-87. <https://doi.org/10.1016/j.jcs.2016.01.001>
- Campuzano A, Rosell CM and Cornejo F (2018) Physicochemical and nutritional characteristics of banana flour during ripening. *Food Chemistry*. 256: 11–17. <https://doi.org/10.1016/j.foodchem.2018.02.113>
- Cardoso JM and Pena RDS (2014) Hygroscopic behavior of banana (*Musa ssp. AAA*) flour in different ripening stages. *Food and Bioprocess Technology* 92: 73–79. <https://doi.org/10.1016/j.fbp.2013.08.004>
- Chang L, Yang M, Zhao N, Xie F et al (2022) Structural, physicochemical, antioxidant and *in vitro* digestibility properties of banana flours from different banana varieties (*Musa spp.*). *Food Bioscience*. 47: 101624. <https://doi.org/10.1016/j.fbio.2022.101624>
- Chávez-Salazar A, Bello-Pérez LA, Agama-Acevedo E, Castellanos-Galeano FJ et al (2017) Isolation and partial characterization of starch from banana cultivars grown in Colombia. *International Journal of Biological Macromolecules* 98: 240–246. <https://doi.org/10.1016/j.ijbiomac.2017.01.024>
- Czekus B, Pećinar I, Petrović I, Paunović N et al (2019) Raman and Fourier transform infrared spectroscopy application to the Puno and Titicaca cvs. of quinoa seed microstructure and perisperm characterization. *Journal of Cereal Science* 87: 25–30. <https://doi.org/10.1016/j.jcs.2019.02.011>
- De Souza AV, de Mello JM, da Silva Favaro VF, dos Santos TGF et al (2021) Metabolism of bioactive compounds and antioxidant activity in bananas during ripening. *Journal of Food Processing and Preservation* 45: e15959. <https://doi.org/10.1111/jfpp.15959>
- Devi K and Haripriya S (2014) Pasting behaviors of starch and protein in soy flour-enriched composite flours on quality of biscuits. *Journal of Food Processing and Preservation* 38: 116–124. <https://doi.org/10.1111/j.1745-4549.2012.00752.x>
- Drapal M, Amah D, Uwimana B, Brown A, Swennen R and Fraser P D (2024) Evidence for metabolite composition underlying consumer preference in sub-Saharan African *Musa spp.* *Food Chemistry* 435: 137481. <https://doi.org/10.1016/j.foodchem.2023.137481>
- Figueroa-Flórez J, Cadena-Chamorro E, Salcedo-Mendoza J, Rodríguez-Sandoval E, Ciro-Velásquez H and Serna-Fadul T (2024) Enzymatic biocatalysis processes on the semicrystalline and morphological order of native cassava starches (*Manihot esculenta*). *Revista Facultad Nacional de Agronomía Medellín*. 77(3): 10839-10852. <https://doi.org/10.15446/rfnam.v77n3.111270>
- Grisi CVB, de Magalhães AMT, de Carvalho AS, Vieira AF et al (2021) Nutritional, anti-nutritional and technological functionality of flour from *Libidibia ferrea*. *Revista Principia-Divulgação Científica e Tecnológica do IFPB* 53: 206-217. <https://pdfs.semanticscholar.org/0717/d97db9da9531e38c573499be39d731c73428.pdf>
- Gutiérrez BL, Márquez-Cardozo CJ and Ciro-Velásquez HJ (2018) Thermodynamic study of adsorption properties of rocoto pepper (*Capsicum pubescens*) obtained by freeze-drying. *Advance Journal of Food Science and Technology* 15: 91–98. <https://doi.org/10.19026/AJFST.14.5877>
- ICONTEC - Instituto Colombiano de Norma Técnica (2020) Harina plátano, banano verde. NTC 2799-2020. Colombia
- Jaramillo-Garcés Y, Sacchet-Pérez M, Manjarres-Pinzon G, Manjarres-Pinzon K et al (2023) Effect of low-temperature storage time on rejected green banana for flour production. *Revista Facultad Nacional*

- de Agronomía Medellín 76: 10517-10526. <https://doi.org/10.15446/rfam.v76n3.105789>
- Khoozani AA, Bekhit AEDA and Birch J (2019) Effects of different drying conditions on the starch content, thermal properties and some of the physicochemical parameters of whole green banana flour. *International Journal of Biological Macromolecules* 130: 938–946. <https://doi.org/10.1016/j.ijbiomac.2019.03.010>
- Kizil R, Irudayaraj J and Seetharaman K (2002) Characterization of irradiated starches by using FT-Raman and FTIR spectroscopy. *Journal of Agricultural and Food Chemistry* 50: 3912–3918. <https://doi.org/10.1021/JF011652P>
- Kumar PS, Saravanan A, Sheeba N and Uma S (2019) Structural, functional characterization and physicochemical properties of green banana flour from dessert and plantain bananas (*Musa* spp.). *Lwt - Food Science and Technology* 116: 108524. <https://doi.org/10.1016/j.lwt.2019.108524>
- López-Ochoa JD, Cadena-Chamorro E, Ciro-Velasquez H and Rodríguez-Sandoval E (2022) Enzymatically modified cassava starch as a stabilizer for fermented dairy beverages. *Starch-Stärke* 74: 2100242. <https://doi.org/10.1002/star.202100242>
- Manjarres-Pinzon G, Castro-Sanchez A, Lopez-Ochoa JD, Gil-Gonzalez J and Rodriguez-Sandoval E (2024) Efectos del reemplazo parcial de harina de trigo con harina de banano verde sobre las propiedades reológicas de la masa y las propiedades de calidad de pan. *Investigación e Innovación en Ingenierías*, 12(1): 45-54. <https://doi.org/10.17081/invinno.12.1.6573>
- Melgarejo LM (2012) *Ecofisiología del cultivo de la gulupa (Passiflora edulis Sims)*. First edition. Universidad Nacional de Colombia, Bogotá. 144p
- Minagricultura - Ministerio de Agricultura y Desarrollo Rural (2021) Sistema de información de gestión y desempeño de organizaciones de cadenas. <https://sioc.minagricultura.gov.co/Banano/Pages/default.aspx>
- Mir SA and Bosco SJD (2014) Cultivar difference in physicochemical properties of starches and flours from temperate rice of Indian Himalayas. *Food Chemistry* 157: 448–456. <https://doi.org/10.1016/j.foodchem.2014.02.057>
- Moravkar KK, Korde SD, Bhairav BA, Shinde SB et al (2020) Traditional and advanced flow characterization techniques: a platform review for development of solid dosage form. *Indian Journal of Pharmaceutical Science* 82: 945-957. <https://doi.org/10.36468/pharmaceutical-sciences.726>
- Ortega Alvarado JE (2016) Estudio de las propiedades fisicoquímicas y funcionales de la harina de banano (*Musa acuminata* AAA) de rechazo en el desarrollo de películas biodegradables (trabajo de grado). Universidad de Ambato, Ambato, Ecuador. 88 p.
- Padhi S and Dwivedi M (2022) Physico-chemical, structural, functional and powder flow properties of unripe green banana flour after the application of refractance window drying. *Future Foods* 5: 100101. <https://doi.org/10.1016/j.fufo.2021.100101>
- Padhi S, Murakonda S and Dwivedi M (2022) Investigation of drying characteristics and nutritional retention of unripe green banana flour by refractance window drying technology using statistical approach. *Journal of Food Measurement and Characterization* 16: 2375–2385. <https://doi.org/10.1007/s11694-022-01349-7>
- Pragati S, Genitha I and Ravish K (2014) Comparative study of ripe and unripe banana flour during storage. *Journal of Food Processing and Technology* 5: 1-6. <https://doi.org/10.4172/2157-7110.1000384>
- Rodríguez-Sandoval E, Franco CML and Manjarres-Pinzon K (2014) Effect of fructooligosaccharides on the physicochemical properties of sour cassava starch and baking quality of gluten-free cheese bread. *Starch/Stärke* 66: 678–684. <https://doi.org/10.1002/star.201300233>
- Salvador LD, Sukanuma T, Kitahara K, Tanoue H and Ichiki M (2000) Monosaccharide composition of sweetpotato fiber and cell wall polysaccharides from sweetpotato, cassava, and potato analyzed by the high-performance anion exchange chromatography with pulsed amperometric detection method. *Journal of Agricultural and Food Chemistry* 48: 3448–3454. <https://doi.org/10.1021/JF991089Z>
- Singh B, Singh JP, Kaur A and Singh N (2016) Bioactive compounds in banana and their associated health benefits - A review. *Food Chemistry* 206: 1–11. <https://doi.org/10.1016/J.FOODCHEM.2016.03.033>
- Stanley R (2017) Commercial feasibility of banana waste utilization in the processed food industry. <https://www.horticulture.com.au/globalassets/laserfiche/assets/project-reports/ba09025/ba09025-final-report-341.pdf>
- Susilo B, Maharani DM, Hawa LC and Fitri DNK (2019) Study of sorption isotherm and isosteric heat of Kepok Banana (*Musa paradisiaca* F.) slice. *IOP Conference Series: Earth and Environmental Science* 230 :012017. <https://doi.org/10.1088/1755-1315/230/1/012017>
- Tribess TB, Hernández-Urbe JP, Méndez-Montevalvo MGC, Menezes EW et al (2009) Thermal properties and resistant starch content of green banana flour (*Musa cavendishii*) produced at different drying conditions. *LWT - Food Science and Technology* 42: 1022–1025. <https://doi.org/10.1016/j.lwt.2008.12.017>
- Vega-Rojas LJ, Londoño-Restrepo SM and Rodríguez-García ME (2021) Study of morphological, structural, thermal, and pasting properties of flour and isolated starch from unripe plantain (*Musa paradisiaca*). *International Journal of Biological Macromolecules* 183: 1723–1731. <https://doi.org/10.1016/j.ijbiomac.2021.05.144>
- Velandia WL (2019) Producción y comercialización de banano en la finca el mango del municipio de Támara Casanare (trabajo de grado). Universidad Santo Tomás. Bogotá, Colombia. 71 p.
- Vogel C, Scherf KA and Koehler P (2018) Effects of thermal and mechanical treatments on the physicochemical properties of wheat flour. *European Food Research and Technology* 244: 1367–1379. <https://doi.org/10.1007/s00217-018-3050-3>
- Wang Y, Zhang M and Mujumdar AS (2012) Influence of green banana flour substitution for cassava starch on the nutrition, color, texture and sensory quality in two types of snacks. *LWT - Food Science and Technology* 47: 175–182. <https://doi.org/10.1016/J.LWT.2011.12.011>
- Wu Z, Ameer K, Hu C, Bao A et al (2022) Particle size of yam flour and its effects on physicochemical properties and bioactive compounds. *Food Science and Technology*. (Brazil) 42: e43921. <https://doi.org/10.1590/fst.43921>
- Zamudio FBP, Vargas A, Gutiérrez F and Bello LA (2010) Caracterización fisicoquímica de almidones doblemente modificados del plátano. *Agrociencia* 44: 283–295. https://www.uaeh.edu.mx/investigacion/icap/LI_IntGenAmb/Juana_Fons/22.pdf